Sl. No.	IIT Ropar List of Recent Publications with Abstract Coverage: February, 2024
1.	A coil rectenna array design to harvest all H-field components for lateral misalignment tolerant wireless powering of bio-medical implant devices **VK Srivastava, A Sharma** - IEEE Journal of Electromagnetics, RF and Microwaves in Medicine and Biology, 2024 **Abstract:** This paper presents a coil rectenna array design to address the lateral misalignment problem in near-field wireless powering of biomedical implants and wearable devices. For this purpose, the proposed design comprises three non-identical orthogonal coil antennas optimized to harvest three orthogonal H-field components efficiently. The rectified energy generated by these antenna units is utilized to supply power to the load by combining the individual rectified output voltages. Out of the two distinct combining techniques, DC and AC combining, DC combining proved advantageous in effectively harnessing the lateral field components. The design parameters of the orthogonal coil rectennas are optimized to enhance the lateral misalignment tolerance area. To realize the proposed rectenna array, a multi-layer PCB technology is employed, resulting in a compact, robust, and cost-effective solution for wireless powering of biomedical implanted and wearable devices. Experimental validation of the analytical results demonstrates that the proposed design has the potential to significantly mitigate the lateral misalignment problem in a 2D plane, achieving a uniformity percentage of 38.18 % for a misalignment tolerance range of 60×60 mm 2 .
2.	A further study on weak byzantine gathering of mobile agents **A Saxena, K Mondal** - ICDCN '24: International Conference on Distributed Computing and Networking, 2024 **Abstract:** The gathering of mobile agents in the presence of Byzantine faults is first studied by Dieudonné et al.. Authors provide a polynomial time algorithm handling any number of weak Byzantine agents in the presence of at least one good agent considering start-up delays, i.e., the good agents may not wake up at the same time. Hirose et al. come up with an algorithm considering start-up delays that use a strong team of at least 4f2 + 8f + 4 many good agents but runs much faster than that of Dieudonné et al.. Later Hirose et al. provide another polynomial time algorithm for gathering in the presence of at least 8f + 8 good agents. However, this algorithm does not work in the presence of start-up delays, also simultaneous termination of good agents is not possible. We, in this work, provide an algorithm considering start-up delays of the good agents reducing the number of good agents w.r.t. Hirose et al. from 4f2 + 8f + 4 to f2 + 4f + 9. Also, our algorithm guarantees simultaneous termination of the good agents.
3.	An efficient approach to obtain analytical solution of nonlinear particle aggregation equation for longer time domains N Yadav, M Singh…**J Kumar**… - Advanced Powder Technology, 2024 **Abstract:** Population balances commonly incorporate physical kernels such as polymerization, generalized bilinear, and Brownian aggregation kernels, which have found widespread application in aerosol physics, astrophysics, chemical engineering, mathematical biology, and pharmaceutical sciences to monitor the dynamics of particles. However, finding analytical solutions for physical relevant kernels over longer time domains in order to validate these models remains a challenging task. The aim of this note is to enhance the semi-analytical solutions obtained from the Adomian decomposition method (ADM) for solving the nonlinear aggregation population balance equation. The applicability of ADM is limited to shorter time domains, and the accuracy of its results decreases as the time domain increases, thereby restricting its potential

	applications. Therefore, a hybrid approach based on ADM and Padé approximant is proposed to find the solutions of the non-linear aggregation equation. The accuracy of the new technique is evaluated by considering Brownian, polymerization and generalized bilinear kernels for which new generalized series solutions are obtained and compared against the finite volume scheme [Kumar et al. (2015), Kinet. Relat. Models 9(2), 373–391]. In addition, the new series solutions for the sum kernel are computed corresponding to a Gamma initial distribution. Quantitative errors in the number density functions are calculated for sum and product aggregation kernels and shown in tables to assess the accuracy of the proposed technique. The results indicate that the new approach provides more accurate analytical solutions for longer time domains while using fewer terms in the truncated series than the ADM and Homotopy perturbation method [Kaur et al. (2019), J. Phys. A: Math. Theor. 52(38), 385201].
4.	An in situ proton filter covalent organic framework catalyst for highly efficient aqueous electrochemical ammonia production KC Ranjeesh…**S Kaur**…**D Gupta**…**TC Nagaiah**… - Advanced Energy Materials, 2024 **Abstract:** The electrocatalytic nitrogen reduction reaction (NRR) driven by renewable electricity provides a green synthesis route for ammonia (NH_3) production under ambient conditions but suffers from a low conversion yield and poor Faradaic efficiency (F.E.) because of strong competition from hydrogen evolution reaction (HER) and the poor solubility of N_2 in aqueous systems. Herein, an in situ proton filter covalent organic framework catalyst (Ru-Tta-Dfp) is reported with inherent Ruthenium (Ru) sites where the framework controls reactant diffusion by suppressing proton supply and enhancing N_2 flux, causing highly selective and efficient catalysis. The smart catalyst design results in a remarkable ammonia production yield rate of 2.03 mg h^{-1} mg_{cat}^{-1} with an excellent F.E. of ≈52.9%. The findings are further endorsed with the help of molecular dynamics simulations and control COF systems without in situ proton filter feasibility. The results point to a paradigm shift in engineering high-performance NRR electrocatalysts for more feasible green NH_3 production.
5.	An orthogonally-polarized multi-beam rectenna system to imitate isotropic DC pattern for orientation-insensitive microwave power delivery **M Kumar, S Kumar, A Sharma, V Malav, P Rattanpal** - IEEE Transactions on Components, Packaging and Manufacturing Technology, 2024 **Abstract:** The Wireless Power Transfer (WPT) rectenna systems suffer from low power conversion efficiency (PCE) due to lower receiver (Rx) gain, polarization mismatch, and angular misalignment that can occur between the transmitter (Tx) and receiver (Rx). This impedes the realization of self-sustaining freely-rotating IoT sensor nodes. To address this issue, an orthogonally-polarized, multi-beam, orientation-insensitive WPT system is proposed to achieve a nearly isotropic DC pattern. The system employs orthogonally-polarized end-fire rectennas (Rect-I & Rect-II) in each sector and a centrally placed cross-polarized patch rectenna (Rect-III) to attain 3D DC coverage. Further, the antenna and rectifier circuit are conjugately matched to achieve miniaturization. A fully integrated hybrid DC combining topology and a smart bypassing network is employed to minimize combining losses. The three rectenna elements offer a PCE of 51 %, 44.9 %, and 58.9 %, with an open-circuit harvested DC voltage of 1600 mV. Thus, orthogonally-polarized, nearly isotropic DC pattern and polarization insensitivity of the proposed multi-beam rectenna system (MBRS) makes it suitable for powering small battery-less IoT sensor nodes.
6.	Analytical formulation of rectenna system performance and fully integrated design for polarization insensitive wireless power transmission **VK Malav, A Sharma** - IEEE Transactions on Microwave Theory and Techniques, 2024 **Abstract:** In wireless power transfer (WPT), rectennas are used as RF-to-dc power converter to recharge the batteries of small Internet-of-Things (IoT) nodes. However, the harvested power of

	the rectenna is affected by the polarization mismatch between the transmitter antenna and the rectenna. The existing rectenna solutions use matching networks (MNs) and hybrid couplers having bulky and lossy elements resulting in degraded power conversion efficiency (PCE). It is unclear which solution is better suited for small IoT nodes. Thus, a mathematical framework is developed for the rectenna performance comparison of the polarization-dependent efficiencies. The efficiency performance for various rectenna designs is formulated and compared. This reveals that the conventional designs are either polarization-sensitive or compromise efficiency. Therefore, a fully integrated and compact linearly polarized multiport rectenna system (N -LPR) is proposed to address the issues. The proposed design does not use MNs and hybrid couplers thus improving the efficiency. Moreover, the performance of the N -LPR is analytically formulated to achieve polarization insensitivity; furthermore, the impact of dc pick location on the rectenna patch is also analyzed. The proposed framework is validated experimentally, and the results demonstrate the feasibility of the proposed rectenna design to accomplish a polarization-insensitive WPT system suitable for recharging small IoT nodes.
7.	Analytical solution of the linearized boussinesq equation considering time-dependent downslope boundary, variable recharge and bedrock seepage **R Sarmah, SR Chavan, I Sonkar** - Water Resources Management, 2024 **Abstract:** The present study proposes an analytical solution to a linearized Boussinesq equation considering unsteady downslope river stage, spatio-temporal rainfall recharge, and bedrock seepage. This analytical solution alleviates the limitations of the previous studies like varying river boundary, leaky aquifer bed, and non-uniform recharge simultaneously. The time-dependent river stage depicts the seasonal water level variation in the river, whereas the leakage from the confined to the unconfined aquifer or vice versa represents the bedrock seepage. The analytical expression is derived using the separation of variable method along with a variable transformation technique. The proposed solution is validated using nonlinear numerical and linearized analytical solution. The study highlights that the aquifers with higher bedrock conductivity tend to have a higher inflow rate to the aquifer from the river during monsoon season and a higher outflow rate to the river from the aquifer in the lean period. The analysis also illustrates that for a relatively flat catchment area, with the rise of the water level in the river, there is a reverse flow from the river to the aquifer. Further, the stream stage variation rate is found to be pivotal in deciding the duration of flow direction alteration and volume of water released from the aquifer. Furthermore, a sensitivity analysis is performed to assess the influence of flow parameters on the discharge function. The discharge is found to be positively sensitive to hydraulic conductivity, aquifer slope, and recharge. Finally, the residence time distributions corresponding to various bedrock seepage conditions are examined. Results indicate that the residence time for the various conditions tends to exhibit the heavy-tailed distributions. © The Author(s), under exclusive licence to Springer Nature B.V. 2024.
8.	Arresting of interfacial phase separation with an imposed flow RX Suzuki, S Seya, T Ban, **M Mishra**, Y Nagatsu - Physical Review Fluids, 2024 **Abstract:** Using fluid displacement in a Hele-Shaw cell, we experimentally demonstrate the arresting effect of an imposed flow on a phase separation occurring in a growing liquid-liquid interfacial region, unlike in an initially homogeneous single-phase mixture quenched within the miscibility gap. Increasing the imposed flow rate reduces the exponent α in the form $\Delta A \propto t^{\alpha}$, where ΔA is the increase in the area occupied by the displacing fluid owing to phase separation. We show that α can be expressed as a function of the ratio of the phase separation rate to the flow rate on a single curve, indicating that the competition between the imposed flow and phase separation rates determines the degree of the interfacial phase separation. The arresting effect and the mechanism are verified by a numerical simulation.
9.	Artificial neural networks with fast transfer learning for statistical signal integrity analysis of MWCNT and MLGNR interconnect networks

	S Guglani…A Dasgupta, **R Sharma**... - IEEE Transactions on Electromagnetic Compatibility, 2024 **Abstract:** In this article, artificial neural network (ANN) metamodels have been developed for the fast statistical signal integrity analysis of multiwalled carbon nanotube and multilayer graphene nanoribbon interconnect networks. These ANN metamodels, referred to as primary ANNs, are trained using transfer learning strategies where the initial guess of the weights and bias terms are learned from a pretrained secondary ANN. The secondary ANN is trained using data extracted from a cheap and approximate equivalent single conductor model of the interconnects. Starting with this informed initial guess, the weights and bias terms of the primary ANN can be optimized using a very small dataset generated from the rigorous but massive multiconductor circuit model of the interconnects. This makes the primary ANN significantly more efficient to train than existing metamodels. Two distinct transfer learning strategies based on the full and partial transfer of knowledge between the primary and secondary ANNs have been developed in this work.
10.	Assessing library professionals' attitude towards information technology applications in three university libraries of North India **TS Handa,** GS Sohal, J Singh - International Journal of Information and Knowledge Studies, 2023 **Abstract:** Purpose: The purpose of the present study is to assess the attitude of library professionals towards information technology (IT) implementation in three university libraries in North India. Methodology: The study uses a survey research method in order to ascertain the attitude of library professionals. The primary data was collected from 91 library professionals (professionals, semi-professionals and para-professionals) through structured questionnaires that were then analyzed using Pearson Chi-square analysis. Findings: The study reveals that there is a positive attitude among library professionals towards the implementation of IT in university libraries. Originality: The study adds value to the current literature on academic libraries in India and is one of the cutting-edge studies to look into library professionals' attitude towards information technology applications in university libraries. Practical implications: The findings suggest that a positive attitude of library professionals was instrumental in implementing the technology in context. However, implementing and maintaining technological infrastructure is an expensive affair that demands investing more funds on the part of university authorities.
11.	Asymptotically correct isoenergetic formulation of geometrically nonlinear anisotropic plates **AK Pathak, SJ Singh, SS Padhee** - Mechanics of Advanced Materials and Structures, 2024 **Abstract:** In the present work, a new displacement-based Equivalent Single Layer (ESL) plate theory has been developed using the Variational Asymptotic Method (VAM) and the principle of isoenergetics. In contrast to the existing assumption-based ESL plate theories, the proposed VAM-based plate theory is devoid of any presuppositions. The VAM decouples the 3D plate problem into a 1D through the thickness analysis and a 2D planar problem. Closed form solutions have been obtained for the 1D problem in terms of 2D displacement variables and their higher-order derivatives. The complexity involving higher-order derivatives of 2D displacement variables has been simplified through the isoenergetic principle ensuring a similar rate of convergence for strains as well as displacements. Solutions for various field variables have been compared against the benchmark problems available in the literature and 3D FEA. These comparisons demonstrate the accuracy, efficiency, and versatility of the present methodology. Key contributions of the present work are (a) First principles-based derivation of the reduced-order 2D plate model from the 3D model energy. (b) The plane stress condition as well as the quadratic variation of transverse shear stress and strain are natural outcomes of the present mathematical framework. (c) This leads to zero tangential traction boundary conditions on the

	plate surface. (d) The effectiveness of capturing higher-order behavior at lower-order results in simplified analysis, reduced computational complexity and increased efficiency. 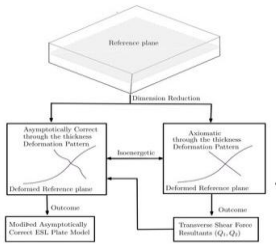
12.	Augmenting the fracture toughness and structural health monitoring capabilities in Kevlar/epoxy composites using carbon nanotubes **D Dhiwar**…. N Gupta, **PK. Agnihotri** - Engineering Fracture Mechanics, 2024 **Abstract:** Timely detection of flaws and improved fracture toughness in Kevlar/epoxy composites is desirable for advanced structural applications. Here, we demonstrate a strategy to simultaneously increase the fracture toughness and damage sensing in Kevlar composites using carbon nanotubes (CNTs). 0.5 wt% CNTs dispersed epoxy is used to fabricate Kevlar/CNT modified epoxy composites. Mechanical testing shows that the CNT addition improves the tensile strength (25 %), interfacial shear strength (16 %), mode I (60 %) and mode II (13 %) fracture toughness of conventional Kevlar/epoxy composites. It is attributed to the toughening of epoxy, stronger interfacial adhesion and crack deflection due to the presence of extremely strong CNTs in modified Kevlar/epoxy composites. High electrical resistance is a major issue to apply resistance based damage sensing techniques in Kevlar/epoxy composites. The conducting network of dispersed CNTs improves through-thickness electrical conductivity of Kevlar/epoxy composites by 6 orders (10-10 to 10-4 S/m) of magnitude. This allows to monitor the crack growth by recording the change in resistance ΔR in CNT modified Kevlar composites. The ΔR-Δa relationship is approximated by a power law $\Delta R=K\Delta a^n$ relation. It is shown that the power law dependence is applicable to a wider class of laminates with varying material dependent parameters K and n. The findings of the present study are a significant in developing in-situ damage sensing strategies for structural composites having high electrical resistance.
13.	Bio-corrosion susceptibility of surface voids and pores in microwave sintered Ti-HAp based bio-composites **R Kumar, A Agrawal** - Materials Letters, 2024 **Abstract:** Deterioration of implants caused by human blood plasma and liquid influence is termed Bio-corrosion. It is detrimental for metal-based implants to function and affects their lifespan adversely. Hybrid-microwave sintered Titanium-Hydroxyapatite-based metal-ceramic composites were studied for corrosion behaviour in Hank's Balanced Salt solution using an electrochemical test in linear polarization potential mode. The sintering induces surface voids and pores, thus its influence on corrosion for Ti-HAp sintered composite was studied. Different corrosion characteristics were determined, and the corrosion sites were analyzed using SEM-EDS. The study could lead to the development of corrosion-resistant porous bio-implants under an actual physiological body-fluid environment.
14.	Biomedical applications of biogenic carbon-based fluorescent nanoparticles **K Kaur, G Singh**, R Badru, N Kaur, **N Singh** - Biogenic Nanomaterial for Health and Environment: Book Chapter, 2023 **Abstract:** The wide-ranging applications of carbon dots (CDs), which can be developed using either green or chemical precursors, have been made possible due to their reported properties and the various precursors that have been identified. This has opened up new opportunities for the development of high-quality CDs and their use in optoelectronic devices, bioimaging, and other

	applications. Green precursors can be derived from fruits, vegetables, flowers, leaves, seeds, stems, crop residues, fungi/bacteria species, and waste products, while chemical precursors can be categorized as either acid reagents or non-acid reagents. It provides a brief review of the past ten years of CD synthesis using both green and chemical precursors, as well as the use of CDs as sensing materials in biomedical applications. This comprehensive review will be a valuable resource for researchers who are interested in synthesizing high-quality CDs for a variety of applications.
15.	Calculation of nuclear matrix elements for 0 ν β β decay of 124 Sn using the nonclosure approach in the nuclear shell model S Sarkar, PK Rath…**RG Pillay**, **PP Singh**…**K Jha**, **PK Raina**... - Physical Review C, 2024 **Abstract:** In this study, we calculate the nuclear matrix elements (NMEs) for the light neutrino-exchange mechanism of neutrinoless double beta decay (0 ν β β) of 124 Sn within the framework of the interacting nuclear shell model, using the effective shell model Hamiltonian GCN5082. The NMEs are calculated employing both closure and nonclosure approaches. For the intermediate nucleus 124 Sb , effects of energy of 100 states for each J π k = 0 + to 11 + and 2 − to 9 − (Δ J k = 1) are explicitly included in the nonclosure approach. The optimal closure energy, which reproduces nonclosure NMEs using the closure approach, is found to be ≈ 3 MeV for 0 ν β β decay of 124 Sn . The NMEs for 0 ν β β decay of 124 Sn did not fully converge with 100 intermediate states for each spin-parity of 124 Sb . A comparison of NMEs and lower limits of T 0 ν 1 / 2 with some of the recent calculations is presented. Further, to gain a comprehensive understanding of the role of nuclear structure on the 0 ν β β decay, the dependence of NMEs on the spin-parity of the intermediate states, coupled spin-parity of neutrons and protons, and the number of intermediate states, is explored. The estimated lower limit on the half-life T 0 ν 1 / 2 ≈ 7.49 × 10 26 yr provides valuable input for the experimental investigations of 0 ν β β decay of 124 Sn in India and elsewhere.
16.	Catastrophic and noncatastrophic population crashes in a bitrophic system with dynamic additional food provision to cooperative predators S Biswas, **A Mandal**, S Pal - Physical Review E, 2024 **Abstract:** In this article we contemplate the dynamics of an additional food-provided prey-predator system. We assume that the behavior of cooperative predators induces fear in prey, which radically affects the prey's birth and death rates. We observe that the structural instability imposed by strong cooperative hunting among predators goes away with higher intensities of fear levels affecting the prey's reproductive output and mortality. High levels of prey refuge are not conducive to the survival of predators. In such a situation, adequate supply of high-quality additional food is favorable regarding the persistence and stability of the system. Interestingly, the system potentially exhibits two stable configurations under identical ecological conditions by allowing different bifurcation scenarios, including saddle-node and backward bifurcations, and associated hysteresis effects with prey refuge along with additional food quantity and quality. In the stochastic environment, the system experiences critical transitions through bifurcation-induced tipping events with time-varying additional food for predators. Enhanced disturbance events promote noise-induced switching and tipping events. Finally, our investigation explores whether impending population crashes resulting from the variability of additional food quantity and quality can reliably be predicted using early warning signals in the context of redshifted noise. Overall, our results may provide insights for finding control strategies in the context of community ecology.
17.	Characterization and performance of co-axial HPGe detectors **SS Kaintura, S Thakur, S Devi, K Tiwari, P Raizada, Amanjot, S Kumar, PP Singh** - Journal of Radioanalytical and Nuclear Chemistry, 2024 **Abstract:** High purity germanium (HPGe) detectors are deployed globally for gamma-radiation

	spectroscopy due to their superior energy resolution. In this work, the essential characteristics of n and p-type HPGe detectors, such as energy resolution, efficiency, minimum detectable activity (MDA), and peak shape were studied for the purpose of characterization and performance optimization. The results are obtained for various source-detector configurations in a wide energy range of 40–1408 keV using gamma sources, such as ^{109}Cd, ^{57}Co, ^{137}Cs, ^{54}Mn, ^{65}Zn, ^{60}Co, and ^{152}Eu. Scanning (distance, lateral, and radial) of the detectors was performed using different gamma sources to understand the orientation of the crystal with its active volume and counting efficiency and to characterize the geometry in detail. The ambient background around the n-type HPGe was reduced using Pb-shielding. As a result, an 85.85% suppression was observed in the mean integral window of 40–2700 keV. The characterization and performance tests of the detectors convincingly suggest that both the detectors can be deployed for environmental radioactivity explorations.
18.	Concept drift challenge in multimedia anomaly detection: A case study with facial datasets **P Kumari, P Choudhary, V Kujur,** PK Atrey, **M Saini** - Signal Processing: Image Communication, 2024 **Abstract:** Anomaly detection in multimedia datasets is a widely studied area. Yet, the concept drift challenge in data has been ignored or poorly handled by the majority of the anomaly detection frameworks. The state-of-the-art approaches assume that the data distribution at training and deployment time will be the same. However, due to various real-life environmental factors, the data may encounter drift in its distribution or can drift from one class to another in the late future. Thus, a one-time trained model might not perform adequately. In this paper, we systematically investigate the effect of concept drift on various detection models and propose a modified Adaptive Gaussian Mixture Model (AGMM) based framework for anomaly detection in multimedia data. In contrast to the baseline AGMM, the proposed extension of AGMM remembers the past for a longer period in order to handle the drift better. Extensive experimental analysis shows that the proposed model better handles the drift in data as compared with the baseline AGMM. Further, to facilitate research and comparison with the proposed framework, we contribute three multimedia datasets constituting faces as samples. The face samples of individuals correspond to the age difference of more than ten years to incorporate a longer temporal context. 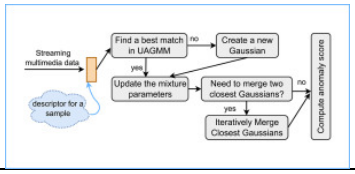
19.	Control of five leg inverter based two motor drive under current sensor failure **A Azeem, AVR Teja, S Payami** - 2023 IEEE International Conference on Power Electronics, Smart Grid, and Renewable Energy (PESGRE), 2024 **Abstract:** This paper proposes a current sensor fault tolerant (CSFTC) control of the five-leg inverter (FLI) that drives the two induction motors independently. The simulation test validation is carried out when all current sensors or power supplies used for current sensor undergo failure. The proposed solution suggests employing generalized equations that leverage the PWM-generated voltage and the angular speed of the rotor. These equations enable the reconstruction of the stator phase current in the stationary reference frame (α-β).This scheme minimizing the system dependency on sensors in noisy environment. The proposed scheme is verified at different operating states of the drive system through the MATLAB/Simulink platform. The simulation result validate the effectiveness and feasibility of proposed scheme.
20.	Copper-catalyzed chemoselective o-arylation of oxindoles: access to cyclic aryl carboxyimidates **PR Singh, M Lamba, A Goswami** - The Journal of Organic Chemistry, 2024

	Abstract: We have developed a highly efficient base- and additive-free chemoselective CuO-catalyzed strategy for the O-arylation of 2-oxindoles to synthesize 2-phenoxy-3H-indole and 2-phenoxy-1H-indole derivatives in the presence of diaryl iodonium salts. This method offers a variety of O-arylated oxindoles in good to excellent yields under relatively milder reaction conditions. Furthermore, this methodology was extended for the O-arylation of 2-pyridinone and isoindoline-1-one derivatives as well. 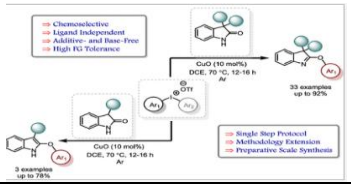
21.	Core-labeled reverse micelle-based supramolecular solvents for assisted quick and sensitive determination of amitriptyline in wastewater **A Sharm , G Singh**, N Kaur, **N Singh** - Langmuir, 2024 **Abstract:** In recent years, the issue of pharmaceutical contaminants in water bodies has emerged as a significant environmental concern owing to the potential negative impacts on both aquatic ecosystems and human health. Consequently, the development of efficient and eco-friendly methods for their determination and removal is of paramount importance. In this context, the development of a surfactant ensemble sensor has been explored for hard-to-sense amphiphilic drug, i.e., amitriptyline. Herein, a pyrene-based amphiphile chemoreceptor was synthesized and characterized through various spectroscopic techniques such as 1H, 13C NMR, single-crystal XRD, FTIR, and ES-mass spectrometry. Then, dodecanoic acid (DA) and a pyrene-based receptor in a THF/water solvent system were used to generate reverse micelle-based self-aggregates of SUPRAS (SUPRAmolecular Solvent). The structural aspects, such as morphology and size, along with the stability of the SUPRAS aggregates were unfolded through spectroscopic and microscopic insights. The present investigation describes a synergistic approach that combines the unique properties of premicellar concentration of supramolecular solvent with the promising potential of pyrene-based receptor for enhanced amitriptyline extraction with simultaneous determination from water (LOD = 12 nM). To evaluate the effectiveness of the developed aggregates in real-world scenarios, experiments were conducted to determine the sensing efficiency among various pharmaceutical pollutants commonly found in water sources. The results reveal that the synergistic nanoensemble exhibits remarkable sensing ability, toward the amitriptyline (AMT) drug outperforming conventional methods. 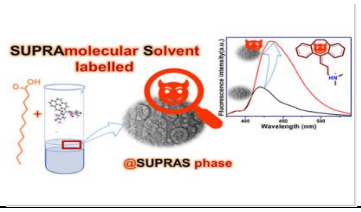
22.	Critical transitions in spatial systems induced by Ornstein–Uhlenbeck noise: spatial mutual information as a precursor **S Deb, PS Dutta** - Proceedings of the Royal Society A: Mathematical, Physical and Engineering Sciences, 2024 **Abstract:** Complex dynamical systems are subject to perturbations across space and time, which can induce a critical transition or tipping in the state of the system. External perturbations are often correlated in time and can interplay with the underlying nonlinearity of the spatial system, affecting the occurrence of critical transitions. Theoretical analysis of the spatial system perturbed by the Ornstein–Uhlenbeck (OU) correlated noise poses challenges beyond the white

	noise assumptions and is yet to be done. Here, we resort to the mean-field approximation of a spatially extended system perturbed with OU noise and obtain the stationary probability density function deriving the Fokker–Planck equation for the same. This allows us to determine the role of diffusion and noise on the resilience of the spatial system. While the theoretical analysis guides us on the landscape of tipping thresholds of the system, critical transitions customary to a variety of systems, require a priori prediction. Here, we propose a probabilistic information-based indicator—spatial mutual information—that can successfully forecast tippings, complementing the previously developed spatial indicators. Further, validating its reliability on empirical data, we show that spatial mutual information serves as a robust indicator capturing information characteristic to an imminent tipping reaching peaks in its vicinity.
23.	Current understanding, motivations, and barriers towards implementing sustainable initiatives in the hospitality industry in the age of automation and artificial intelligence A B Singh, G Gaurav, **P Sarkar**… - Recent Patents on Engineering, 2024 **Abstract:** Background: Sustainability concerns are rapidly being acknowledged as a key concern for hospitality sectors worldwide. Sustainable initiatives immediately contribute to improved organizational performance in terms of utility consumption, waste management, and regulatory compliance, resulting in cost-effectiveness and competitive advantage through distinctiveness. Objective: The purpose of the patent study is to analyze and summarize the motivations, indicators, and barriers towards applications of sustainable initiatives and modern technologies in the hospitality industry using the existing literature to develop a current understanding of the subject and know the way the current industry is thinking about it. Method: This study is a combination of systematic and bibliometric review, where the systematic review was based on selected articles from reputed journal databases, and the bibliometric review was conducted using VOS viewer and web of science database for a period of 20 years (2002-2022) Seven research questions were framed and answered for the systematic review. Result: By describing the motivations, barriers, and impacts of implementing sustainability initiatives and cutting-edge technologies like AI and machine learning in the hospitality sector, the study helps practitioners and academics understand its present state for robust research. The current condition of such implantations in the hospitality sector is also discussed. Conclusion: This study adds value by shedding light on the perspective of sustainability in the hospitality industry by considering the recommendations and practical advice for hotel management suggested in the existing literature about the application of current sustainability innovations and effective sustainability initiatives in hotel management.
24.	Design and implementation of load network time constant computation based solar active power filters cum injector for industrial loads/grids **PM Reddy, BK Gupta, KR Sekhar** - IEEE Access, 2024 **Abstract:** This work proposes an efficient integration method of solar energy with industrial nonlinear loads, accounting for dynamic variations in solar power and load harmonic profiles. The involved dynamics necessitate that the solar interface front-end inverters be equipped to handle both harmonic distortions and active power injection characteristics simultaneously. In this work, an instantaneous load and source characteristic mapping is proposed for the solar-interfaced front-end inverter operated as a shunt active power filter cum active power injector in order to accommodate the dynamic variations of the source and load. As per requirement, to separate the load-demanded and switching harmonics, a new load network time constant-based passive filter design diverging from traditional passive filter design methods is demonstrated. Further, a comprehensive explanation of the current controller modeling methodology is elaborated, considering the essential bandwidth required for proficiently managing load-demanded harmonics in both grid injection and drawing modes of operation. Later, in grid injection mode, the influence of grid and system impedance interactions on the power quality is analyzed for weak grid scenarios to derive the requisite bandwidth conditions to ensure resilient

	power transfer. Subsequently, the experimental validation of the solar interfaced shunt active power filter (SISAPF) with active power injection capability is carried out in both grid power drawing and injection modes, demonstrating the effectiveness of the enhanced bandwidth in handling load-demanded harmonics and solar power dynamic variations
25.	Design optimization of 20/16 outer rotor five phase switched reluctance motor for ev application **Z Rayeen, S Payami** - 2023 IEEE International Conference on Power Electronics, Smart Grid, and Renewable Energy (PESGRE), 2024 **Abstract:** The outer rotor switched reluctance motor (OR-SRM) is a favorable choice for electric vehicle (EV) applications due to its high torque density, power density, robustness, low cost and low maintenance requirements. However, its usability in EVs is limited by inherent torque ripple and a low power factor. These drawbacks can be mitigated by increasing the number of motor phases. This research paper introduces a outer rotor five-phase (OR-FPSRM) switched reluctance motor with a 20/16 slot-pole configuration designed for EV applications. The study includes a parametric analysis of geometric parameters such as bore diameter and stack length, examining their impact on performance. This analysis assists designers in selecting the optimal tuning variables for the motor. To optimize the design of the OR-FPSRM, a genetic algorithm (GA) is employed. The torque and copper loss are used as the cost functions for the optimization process. The paper presents the results of the optimization solution and the performance of the OR-FPSRM under both rated and variable load conditions.
26.	Development and characterization of gelatin/carboxymethyl cellulose based polymeric film with inclusion of ionic liquid to enhance the shelf life of food **A Singh**, J Singh, **N Singh**, N Kaur - Food Packaging and Shelf Life, 2024 **Abstract:** Gelatin is the key biopolymer with the potential uses in numerous sectors since it is biodegradable and biocompatible. But for instance, food packaging material gelatin itself is not so stable and flexible. In order to overcome this drawback, we have constructed a carboxy methyl cellulose (CMC) and gelatin-based polymeric films at a temperature of 55 °C. A polymeric film with the addition of ionic liquid (IL), shows tremendous antibacterial and antioxidant properties towards food packaging. Ionogel films show different properties with different compositions of ionic liquid (IL0%, IL5%, and IL20%). The characterization of prepared polymeric films has been carried out for their surface morphology, thermal stability, UV shielding, optical properties, smoothness, and antimicrobial properties. The antibacterial activity of polymeric film (PF@IL20%) was tested on both Gram-negative E. coli (Escherichia coli) and Gram-positive S. aureus (Staphylococcus aureus) bacteria. In particular, PF@IL20% exhibits potent activity against E. coli and S. aureus with MIC values of 7 ± 2 μg mL−1 and 13 ± 2 μg mL−1 respectively. It was observed that ionogel matrix shows excellent antibacterial and antioxidant properties toward food packaging and their antibacterial mechanism was explored by SEM and AFM analysis. Further, ionogel PF@IL20% was applied for food (red apple) packaging abilities and with inclusion of 20% ionic liquid exhibited exceptional food wrapping applicability, which increases the shelf life of red apples by preventing air-oxidation. 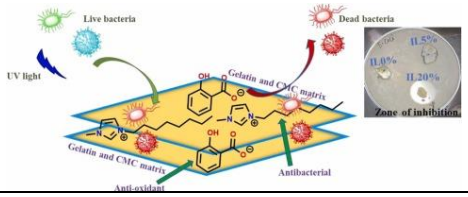
27.	Do different credit flows affect the current account differently? evidence from emerging economies **B Garg**, H Paranavithana - Emerging Markets Finance and Trade, 2024

	Abstract: This paper examines the impact of credit flows, both at the aggregated and disaggregated level, on current account balances for five Southeast Asian economies. Evidence shows that total credit flows improve the current account position, especially in India and Indonesia, in the presence of adequate financial development. Nevertheless, for China, we find that credit flows lead to a decline in current account balances. When disaggregating the total credit flows, in the case of China, we find that household credit negatively influences the current account balance while the bank and business do not have any significant effect. Similarly, for India, we find that most of the improvement in the current account from credit flows comes from household and bank credit. Interestingly, in the case of Indonesia, Malaysia, and Thailand, we find evidence of aggregation bias. The asymmetric impact of disaggregated credit flows implies that policy prescriptions based on aggregate credit flows may be ill-advised and macroeconomic policymakers must implement targeted measures for different types of credit.
28.	Effect of carbon sequestration methods on uptake potential and characteristics of ordinary portland cement-based concrete **SK Saikia, AS Rajput** - Construction and Building Materials, 2024 **Abstract:** Cementitious concrete is considered potentially the largest avenue to utilize the captured carbon dioxide (CO2). Its capacity is significantly influenced by various parameters, including the CO2 introduction method for sequestration. This paper attempted to study the variation in carbon sequestration potential of ordinary Portland cement (OPC) based concrete and paste when the CO2 is introduced to the samples during mixing, curing and both. The carbonated samples obtained using the abovementioned methods have been compared in terms of CO2 uptake capacity, microstructural densification, porosity reduction, and strength variations. A maximum CO2 Uptake Capacity of about 25% was achieved under Standard Ambient Temperature and Pressure (SATP) conditions, with a maximum CO2 Conversion of 70.35% and 93.80% obtained at the surface for CO2 Mixing and CO2 Curing, respectively. Further, carbon-sequestered concrete (CSC) resulted in enhanced compressive strength, and reduced the size of pores in addition to making them uniform in size.
29.	Effect of eccentricity on electro-thermal runaway in the insulation of extruded high voltage DC cables **P Johri, CC Reddy** - IEEE Transactions on Dielectrics and Electrical Insulation, 2024 **Abstract:** This paper presents the electro-thermal runaway characteristics of an extruded high voltage direct current (HVDC) cable, in the presence of eccentricity, i.e., a misalignment in the axes of cable conductor and insulation, which is practically unavoidable in extruded cables. In particular, eccentricity in DC case assumes importance due to non-linear, temperature (or load current) dependent field dynamics as compared to alternating current (AC) case. Effect of eccentricity on electro-thermal breakdown has not received adequate attention till now. In this work, the authors simulate the runaway in a HVDC cable and investigate the impact of eccentricity under different scenarios such as short-time and long-time instability, using a comprehensive FEM model. The results show a drastic shift in phenomenon from traditional global thermal breakdown to local thermal breakdown due to eccentricity in power cables. The results are validated with analytical computations.
30.	Effect of ultrafine-grained structure and chromium addition on corrosion resistance of Ni-Cr-Al alloys **D Singh**, H K Mehtani, **R Kumar**… - Materials Characterization, 2024 **Abstract:** The present work aims to understand the various scientific aspects related to the corrosion behavior of the ultrafine-grained (UFG) and coarse-grained (CG) Ni-(10,20)Cr-10Al (wt%) alloys in 3.5 wt% NaCl solution based on the passive layer formation on the alloys. In this regard, UFG and CG Ni-(10, 20)Cr-10Al (wt%) alloys were synthesized and characterized. Results of corrosion studies reveal that the UFG structure of the alloys is favorable to enhance

	the corrosion performance due to their high grain boundary density, which provides nucleation sites for rapid and effective passivation of the alloys by the formation of external Cr2O3 layer instead of mixed oxides/hydroxides. Besides, the Cr addition to the alloys also fosters the Cr-containing passive layer formation. The superior corrosion behavior of the UFG alloys is supported by scanning electron microscopy, electrochemical impedance spectroscopy, and Raman spectroscopy. 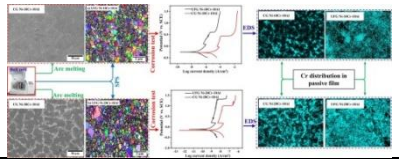
31.	Elastoviscoplasticity intensifies the unstable flows through a micro-contraction geometry **A Chauhan, C Sasmal** - Journal of Non-Newtonian Fluid Mechanics, 2024 **Abstract:** This study focuses on the two-dimensional numerical investigation of complex fluid flows through a micro-contraction geometry in the creeping flow regime, specifically examining elastoviscoplastic (EVP) fluids. These fluids exhibit a combination of viscous, elastic, and plastic behaviors. The governing equations, including mass and momentum, are solved using a finite volume method-based discretization technique. Saramito's constitutive model is utilized to accurately represent the viscous, elastic, and plastic responses of the EVP fluid. The present results demonstrate significant differences in flow dynamics, such as vortex dynamics and transitions between flow regimes (e.g., steady to unsteady), when compared to simple Newtonian and non-Newtonian viscoelastic (VE) or viscoplastic (VP) fluids. This study reveals that when the yield strain exceeds a critical value, approximately ranging from 0.79 to 0.89, the flow transits from a steady to an unsteady state for the EVP fluids. Importantly, the present study shows that EVP fluids exhibit intensified chaotic flow dynamics and increased instability compared to VE and VP fluids under similar flow conditions. However, the presence of shear-thinning behavior in EVP fluids suppresses this instability. The analysis of local velocity fields and flow deformation in this study highlights the impact on the stretching of fluid microstructure and elastic stresses, which ultimately contribute to the origin of this intensified unstable flow condition for EVP fluids. The finding from this study holds significant potential for enhancing heat or mass transfer rates and mixing efficiency in micro-scale systems, where the prevailing steady and laminar flow conditions often hinder these transport processes.
32.	Electrochemical oxidative dearomatization strategy for accessing spiro[4.5]dienones and derivatives **R Bag, NP Mishra, D Saha, P Banerjee** - The Journal of Organic Chemistry, 2024 **Abstract:** Electrochemical dearomatization has been recognized as an attractive tool for the rapid construction of structurally diverse molecules. The designed methodology encompasses an eco-friendly and efficient electrochemical approach to synthesizing spiro[4.5]dienones under mild reaction conditions. Furthermore, detailed mechanistic studies strongly bolster our hypothesis and emphasize the role of HFIP in the mechanism. The protocol is scalable and showcases a broad substrate scope with tolerance toward numerous functional groups. Henceforth, this strategy can be deployed as an alternative and sustainable tool for accessing spiro[4.5]dienones. 
33.	Entanglement and chaos near critical point in strongly coupled gauge theory D Karan, **S Pant** - The European Physical Journal C, 2024

	Abstract: We perform a holographic study of the high and low temperature behaviours of logarithmic negativity (LN) and entanglement wedge cross section (EWCS) in a large N strongly coupled thermal field theory with critical point, having a well defined gravity dual known as 1RC black hole. The bulk theory accommodates a dimensionless parameter , proportional to the charge of the 1RC black hole. Holographically, limit ensures an existence of a critical point in the dual boundary theory. We show that the logarithmic negativity in low and high temperature limits enhances with increasing . We analytically compute the EWCS in low and high temperature limits and find an agreement with the previously reported numerical results. We holographically explore the correlation between two identical copies of thermal field theory with critical point forming a thermofield double state (TFD) by computing the thermo mutual information (TMI). TMI shows an increasing behaviour with respect to the width of the boundary region. Furthermore, we study the chaotic behaviour of the field theory by analyzing a shock wave in the dual eternal 1 RC black hole and then estimate the degradation of TMI. The rate of such disruption of TMI slows down as the value of critical parameter takes higher values.
34.	ENVINet5 deep learning change detection framework for the estimation of agriculture variations during 2012–2023 with Landsat series data G Singh, N Dahiya, **V Sood**… - Environmental Monitoring and Assessment, 2024 **Abstract:** Remote sensing is one of the most important methods for analysing the multitemporal changes over a certain period. As a cost-effective way, remote sensing allows the long-term analysis of agricultural land by collecting satellite imagery from different satellite missions. Landsat is one of the longest-running world missions which offers a moderate-resolution earth observation dataset. Land surface mapping and monitoring are generally performed by incorporating classification and change detection models. In this work, a deep learning-based change detection (DCD) algorithm has been proposed to detect long-term agricultural changes using the Landsat series datasets (i.e., Landsat-7, Landsat-8, and Landsat-9) during the period 2012 to 2023. The proposed algorithm extracts the features from satellite data according to their spectral and geographic characteristics and identifies seasonal variability. The DCD integrates the deep learning-based (Environment for visualizing images) ENVI Net-5 classification model and posterior probability-based post-classification comparison-based change detection model (PCD). The DCD is capable of providing seasonal variations accurately with distinct Landsat series dataset and promises to use higher resolution dataset with accurate results. The experimental result concludes that vegetation has decreased from 2012 to 2023, while build-up land has increased up to 88.22% (2012–2023) for Landsat-7 and Landsat-8 datasets. On the other side, degraded area includes water (3.20–0.05%) and fallow land (1–0.59%). This study allows the identification of crop growth, crop yield prediction, precision farming, and crop mapping.
35.	Estimation of radionuclides in the soil samples from the uranium mining zone of Sikar, Rajasthan, India B Khyalia…**SS Kaintura, PP Singh**… - Journal of Radioanalytical and Nuclear Chemistry, 2024 **Abstract:** The presence of underlying uranium deposits may contaminate the upper soil of a region. We have carried out a detailed investigation of radionuclides (Ra, Th, and K) present in the soil around the reported uranium deposit site in the Sikar district of Rajasthan, India. Measurements are carried out using the state-of-the-art gamma-ray spectroscopy (HPGe detector) technique. The specific activity of 226Ra, 232Th, and 40K are found in the range of 9.5 ± 0.5–50.6 ± 1.0 Bq kg−1, 11.0 ± 0.4–83.2 ± 1.5 Bq kg−1, and 177 ± 13–753 ± 47 Bq kg−1 with the mean values of 17.8 ± 7.5 Bq kg−1, 22.6 ± 13.4 Bq kg−1, and 393 ± 76 Bq kg−1 respectively. The average value of Ra Eq. activity is 80.4 Bq kg−1, below the recommended limit of 370 Bq kg−1. For radiological implications in the study area, the indoor and outdoor absorbed dose rates and age-dependent annual effective dose are estimated, which are also found below their

	prescribed safe limit values. The mean value of other hazard indices (Hin and Hex) and level indices (Iα and Iγ) are less than unity. Our study shows that the underlying uranium deposits do not contaminate the soil of the studied area and the soil is safe to use for various purposes.
36.	Eternal connected vertex cover problem in graphs: complexity and algorithms **K Paul, A Pandey** - Algorithms and Discrete Applied Mathematics, 2024 **Abstract:** A variation of the vertex cover problem is the eternal vertex cover problem. This is a two-player (attacker and defender) game, where the defender must allocate guards at specific vertices in order for those vertices to form a vertex cover. The attacker can attack one edge at a time. The defender must move the guards along the edges so that at least one guard passes through the attacked edge (guard moves from one end point of the attacked edge to the another end point), and the new configuration still acts as a vertex cover. If the defender is unable to make such a maneuver, the attacker prevails. If a strategy for defending the graph against any infinite series of attacks emerges, the defender wins. The eternal vertex cover problem is to find the smallest number of guards with which the defender can develop a successful strategy. The same problem is referred as the eternal connected vertex cover problem if the following additional requirement is added: underlying vertices of each defensive configuration form a connected vertex cover. The smallest number of guards that can be used to create a successful defensive strategy, in this case, is known as the eternal connected vertex cover number and is denoted by the ecvc(G). The decision version of the eternal connected vertex cover problem is NP-hard for general graphs and it also remains NP-hard for bipartite graphs. In this paper, we proved that the problem is polynomial-time solvable for chain graphs and cographs. In addition, we proved that the problem is NP-hard for Hamiltonian graphs, and proposed a polynomial-time algorithm to compute eternal connected vertex cover number for Mycielskian of a given Hamiltonian graph.
37.	Experimental investigation of micro-pillar textured WC inserts during turning of Ti6Al4V under various cutting fluid strategies S Gaurav, **CK Nirala** - Journal of Manufacturing Processes, 2024 **Abstract:** Continuous shearing of the chip under the condition of seizure at the chip/tool interface has been recognized as a major source of heat input to the tool. This heat is unsafe for the tool life as it exhibits high plastic deformation of the sharp cutting edge under the action of high compressive stresses, leading to flank and crater wear. To diminish the severity of this condition, it seems impelling to decrease the chip/tool interface contact and enhance cutting fluid (air/liquid) penetration and retention into this seizure zone. Surface texturing of cutting tools has been gaining popularity in this aspect. This work extensively studies a turning operation using innovative textures fabricated using the Reverse Micro Electrical Discharge Machining (RμEDM) process on the tool surface. These textures, in the form of arrayed micro-pillars, were tested under dry, compressed air, MQL, and wet conditions during the turning of Ti6Al4V. The objective is to understand the ability of these micro-pillars to influence the cutting action in terms of tool wear, contact area, severity of adhesion, surface roughness of the work material, and chip morphology. It is visible from the overall experimental results that the textured pattern has the potential to decrease the chip/tool contact area by promoting tighter curling of the chips. A maximum of 52.3 % reduction in chip curl radius is achieved under compressed air condition. The textures assist in reducing the intensity of adhesion as high as 68.22 % on the chip/tool interface under dry machining and, hence, the temperature input to the tool. A similar deduction can be made from the reduced flank wear width with a maximum reduction of 18.45 % under wet conditions, indicating prolonged sharpness retention of the cutting edge. The measured feed forces also concur with the reduced contact area at the interface. A reduction of 30.96 % in the contact area is achieved, corresponding to a 19.73 % reduction in feed force under wet machining condition.

	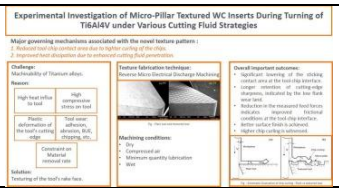
38.	Exploiting n-centered umpolung reactivity of α-iminomalonates for the synthesis of n-sulfenylimines and sulfonamides **S Roy**…**A Chakraborty, I Chatterjee**... - Organic Letters, 2024 **Abstract:** An efficient and interesting N-centered umpolung method has been disclosed to construct beneficial S–N bonds, furnishing N-sulfenylimines, which can readily be converted into the corresponding sulfonamide derivatives in a one-pot sequential operation. N-Sulfenylimines are potent intermediates in organic synthesis, whereas sulfonamides are of major molecular interest due to their rich biological activities and wide applicability in medicinal chemistry. Owing to the simple reaction conditions and setup, this protocol displays a broad and versatile substrate scope, resulting in excellent functional group tolerability toward the synthesis of both N-sulfenylimines and sulfonamides. A density functional theory (DFT) computed and experimentally supported convenient mechanism has been proposed for this unique method. 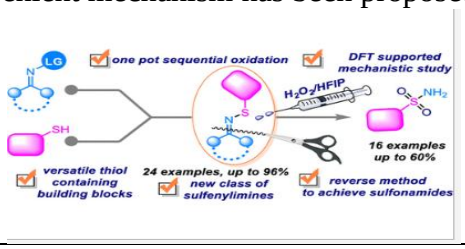
39.	Force and motion analysis of blade-less wind energy harvesters **KK Verma, AVR Teja** - 2023 IEEE International Conference on Power Electronics, Smart Grid, and Renewable Energy (PESGRE), 2024 **Abstract:** This paper is focused on design of blade-less wind energy harvesters(BWEH) and computational fluid dynamic analysis of BWEH. Conventional wind turbine uses rotary machines to extract power from wind which requires high maintenance and the wake area between two wind turbines is significantly large. In contrast to conventional wind turbines, which rely on rotary mechanisms for power generation, bladeless turbines extract the energy procured from vortex-induced vibrations(VIV). Mathematical model equation are developed using dimensional analysis. Nature of lift force experienced by the BWEH, Motion of blade-less wind energy harvester is discussed in the paper.
40.	Graph embedded intuitionistic fuzzy random vector functional link neural network for class imbalance learning **MA Ganaie,** M Sajid, AK Malik ... - IEEE Transactions on Neural Networks and Learning Systems, 2024 **Abstract:** The domain of machine learning is confronted with a crucial research area known as class imbalance (CI) learning, which presents considerable hurdles in the precise classification of minority classes. This issue can result in biased models where the majority class takes precedence in the training process, leading to the underrepresentation of the minority class. The random vector functional link (RVFL) network is a widely used and effective learning model for classification due to its good generalization performance and efficiency. However, it suffers when dealing with imbalanced datasets. To overcome this limitation, we propose a novel graph-embedded intuitionistic fuzzy RVFL for CI learning (GE-IFRVFL-CIL) model incorporating a weighting mechanism to handle imbalanced datasets. The proposed GE-IFRVFL-CIL model offers a plethora of benefits: 1) leveraging graph embedding (GE) to preserve the inherent

	topological structure of the datasets; 2) employing intuitionistic fuzzy (IF) theory to handle uncertainty and imprecision in the data; and 3) the most important, it tackles CI learning. The amalgamation of a weighting scheme, GE, and IF sets leads to the superior performance of the proposed models on KEEL benchmark imbalanced datasets with and without Gaussian noise. Furthermore, we implemented the proposed GE-IFRVFL-CIL on the Alzheimer's Disease Neuroimaging Initiative (ADNI) dataset and achieved promising results, demonstrating the model's effectiveness in real-world applications. The proposed GE-IFRVFL-CIL model offers a promising solution to address the CI issue, mitigates the detrimental effect of noise and outliers, and preserves the inherent geometrical structures of the dataset.
41.	Impact of ion-specific interactions on laser-induced liquid microjet generation **B Rana, R Kamath, M Mishra, KC Jena** - Physics of Fluids, 2024 **Abstract:** Jet velocity and jet power are the crucial parameters that govern the release profile of drugs/vaccines in needle-free injection systems, where salts are considered as one of the essential constituents of drugs/vaccines as adjuvants. However, the impact of salts on the generation of laser-induced liquid microjets that have shown tremendous potential for drug delivery has remained unexplored. Here, we have investigated the influence of Hofmeister ions on the velocity of laser-induced liquid jets in rhodamine 6G (Rh6G) dye solution. A comprehensive experimental approach is adopted to find out the values of the liquid microjet velocity by varying the parameters, such as input energy of the laser beam, concentrations of the dye, and specific Hofmeister ions in the aqueous solution. From our experimental findings, it is observed that the presence of ions significantly influences the jet velocity that follows the Hofmeister series: . This, in turn, governs the ion-specific penetration depth of liquid jets as simulated for the model soft tissues. The observed Hofmeister trend in the jet velocity values showcases the possible specific-ion interactions between anions and Rh6G molecules in the aqueous solution. Our detailed experimental findings on ion-specific jet velocity and jet power could be beneficial in designing needle-free drug delivery systems with controlled penetration depths.
42.	Integral mean estimates for univalent and locally univalent harmonic mappings S Das, **AS Kaliraj** - Canadian Mathematical Bulletin, 2024 **Abstract:** We verify a long-standing conjecture on the membership of univalent harmonic mappings in the Hardy space, whenever the functions have a "nice" analytic part. We also produce a coefficient estimate for these functions, which is in a sense best possible. The problem is then explored in a new direction, without the additional hypothesis. Interestingly, our ideas extend to certain classes of locally univalent harmonic mappings. Finally, we prove a Baernstein-type extremal result for the function $\log(h'+cg')$, when $f=h+g$ is a close-to-convex harmonic function, and c is a constant. This leads to a sharp coefficient inequality for these functions.
43.	Investigation into hydrogen assisted fracture in nickel oligocrystals V Singh, A Raj, **DK Mahajan** - Materials Science and Engineering: A, 2024 **Abstract:** This study investigates the hydrogen embrittlement (HE) behavior of Nickel-201 alloy using the oligocrystal approach. To comprehend the influence of microstructure toward HE, various types of tensile oligocrystals (True-oligocrystals, Quasi-oligocrystals, Identical-oligocrystals, and Bi-crystal type oligocrystals) with diverse microstructure (in terms of Schmid factor distribution and grain boundary types) are generated using a combination of heat treatment and slicing method. The electron backscatter diffraction (EBSD) analysis is used to validate the development of the desired tensile oligocrystal samples. Identical oligocrystal samples established the transition in fracture mode from ductile transgranular (TG) to brittle intergranular (IG), solely driven by hydrogen uptake. Post-tensile deformation analysis validated the hydrogen-induced IG fracture initiation and propagation along the random high-angle grain boundaries (RHAGBs) only. Bi-crystal type oligocrystals with low angle grain boundaries (LAGBs) and coincident-site lattice (CSL) 3 grain boundaries exhibited resistance to hydrogen-induced

	intergranular fracture, thus establishing the 'special' nature of these grain boundaries against the HE under current testing conditions.
44.	Investigation of hydrogen transport properties through the liner material of 70 MPA type iv composite overwrapped pressure vessels **M Kumar** - International Journal of Pressure Vessels and Piping, 2024 **Abstract:** In zero-emission solutions for the hydrogen supply chain, high-pressure hydrogen storage in Type IV composite overwrapped pressure vessels (COPVs) is crucial for being safe and secure for a variety of stationary and transport applications. These COPVs consist of a polymeric liner material that works as a barrier for the stored hydrogen, while the carbon fiber-based composite provides the strength to hold the high-pressure hydrogen (of nominal working pressure more than 70 MPa to achieve the competitive driving range). Several experimental studies and simulation work have been performed on the viability of various polymers as low-permeability materials under low-pressure conditions. However, because of their proprietary nature and commercialized research, the characteristics of hydrogen permeation through polymers and their behavior at high pressure are still readily available in the literature. It is a major concern and the most crucial component of Type IV COPVs that these polymeric liners hold high pressure and maintain the necessary density of hydrogen (state of charge) toward operational requirements and safety concerns related to the cause of failures due to permeation (such as blistering, buckling, cracking, and so on). This paper investigates the role of polymeric liners on hydrogen permeation behavior using finite element modeling. For this, a UMATHT subroutine is developed within the Abaqus software to implement a new hydrogen permeation transport model with extended governing equations. Through the simulations and material modeling, the role of hydrogen transport properties (permeability, diffusivity, and solubility), structural characteristics (crystallinity, free volume, thickness) of plastic liners, and the role of operational parameters (concentration, pressure) are combined to validate the model from the experimental data in the literature to estimate the effective thickness required to maintain the permeation limit of the polymeric liner of 70 MPa Type IV COPVs.
45.	Kinetic and mechanistic way for photocatalytic degradation of pollutants from textile wastewater by graphene oxide supported nanocomposite A Das, **MK Adak** - Next Materials, 2024 **Abstract:** Textile wastewater is the primary origin of wastewater and exposes tremendous toxicity to the ecosystem. The participation of massive water quantities in the various steps of textile treatment and their free release disrupts the ecological functions of living creatures. A heterogeneous photocatalyst with nontoxicity, strong oxidizing ability, broad scale of pH functionality, stable structure, and low-cost value is highly challenging for the application purpose. Graphene oxide (GO) and semiconductor materials-based composite show high performance in the photocatalytic process for wastewater treatment. The π-π stacking, electrostatic, and hydrogen bonding interaction between graphene and the organic pollutants leads to more pollutant adsorption, reflecting high degradation efficiency. Again, the electron conduction bridge, interfacial mediator, and photosensitizer role of the GO enhances the charge separation efficiency of the reactive species. In such cases, the Z-scheme, S-scheme mechanistic path, and the involvement of reactive oxygen species (ROSs) are very important in studying the reason behind the high performance of the composite. This review article discusses the textile toxic wastewater outcome on human wellness, the functionality of the graphene-based material, the wide range of light absorption capability, ROSs generation, the charge recombination process, kinetic and mechanistic pathway, and the advanced technology for a better approach in the future.
46.	MARS: A multiview contrastive approach to human activity recognition from accelerometer sensor **G Sharma, A Dhall**, R Subramanian - IEEE Sensors Letters, 2024

	Abstract: In this letter, we present MARS, a novel approach, which com-bines a multiview fusion technique with contrastive loss to accurately identify human activities using accelerometer sensor data. Accelerometer sensor enables precise monitoring of human activities in diverse contexts. Our approach leverages both temporal and spectral views of accelerometer data, integrating them through an attention mechanism to enhance the overall understanding of human activities. To further improve the discriminative power of the learned representations corresponding to different activity classes, we apply a contrastive loss-based siamese network. Emprical findings confirm that MARS outperforms state-of-the-art on the harAGE dataset by a significant margin of 4.71 in unweighted average recall.
47.	Microkinetic modeling of furan hydrodeoxygenation over transition-metal surfaces **DR Kanchan, A Banerjee** - The Journal of Physical Chemistry C, 2024 **Abstract:** Hydrodeoxygenation (HDO) of biomass-derived oxygenates present in bio-oil is a critical step in their conversion to high-value chemicals and fuels. Furanics represent a significant fraction of the bio-oil and are considered as potential platform chemicals to yield a variety of valuable chemicals. In this study, density functional theory calculations and a descriptor-based microkinetic modeling (MKM) approach were utilized to investigate furan HDO on transition-metal surfaces and predict activity and selectivity for the formation of ring-hydrogenated product like dihydrofuran (DHF), open-chain alcohols, aldehydes, and deoxygenated molecules as a function of carbon (EC) and oxygen-binding energies (EO). Deoxygenated products were favored at high temperatures and low pressures on surfaces with weak EC and strong EO, while alcohols were favored on surfaces with weak EO and low temperatures. DHF and aldehyde formation were favored at high H2 pressures and low temperatures on surfaces having very weak oxygen-binding energies and very high carbon/oxygen-binding energies, respectively. Ni had high activity and selectivity toward deoxygenated products in agreement with experimental observations, while Pd and Pt show the highest activity and selectivity toward ring-hydrogenated products. Our MKM analysis was extended to screen single-atom alloy surfaces for HDO activity, and NiFe was found to be a potential deoxygenating catalyst in agreement with previous experimental studies. 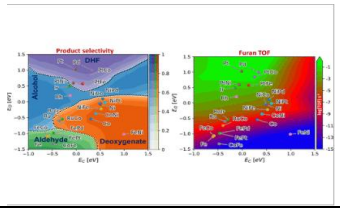
48.	Mixing dynamics in the synthesis of nanoparticle-stabilized water-in-water emulsion: Impact on size and stability **C Shekhar, VS Pawak, V Mehandia**…**M Sabapathy**... - Physics of fluids, 2024 **Abstract:** This communication presents a comprehensive investigation into the impact of mixing on the synthesis of water-in-water Pickering emulsions. The approach employs commercial-grade oppositely charged nanoparticles within two distinct fluid phases, facilitating self-assembly and the formation of aggregates with variable sizes and compositions. Enhanced interfacial area, achieved through aggregate adsorption at the interface, elevates the Gibbs detachment energy of particles between the two aqueous phases, leading to stable emulsion formation. We further explore the effect of various mixing devices, including high-pressure and sonic wave mixing. Our findings reveal that mixing within the aqueous phase critically influences emulsion size, with sonicator-assisted mixing producing smaller droplets than homogenizer mixing. Both devices yield poly-dispersed droplet size distributions. Interestingly, the droplet size correlates well with the Hinze scale (hd), and the Kolmogorov length scale (ld) exhibits good correspondence within a specific operating range. The proposed method introduces a streamlined, one-step synthesis

	process for easy preparation, demonstrating excellent stability for a minimum of 30 days. This study pioneers the investigation of mixing effects within an aqueous two-phase system utilizing a Pickering emulsion template.
49.	Modeling of 2D thermo-elastic brittle fracture using smoothed floating node method **U Singh, S Kumar,** H Pathak... - Mechanics of Advanced Materials and Structures, 2024 **Abstract:** This paper presents an extension of the recently developed smoothed floating node method (SFNM) with cohesive zone approach to model crack growth in elastic materials under thermo-elastic loading conditions. The SFNM utilizes floating nodes to accurately model the crack by activating dormant nodes at intersection points of crack path and the corresponding element edges. Through the activation of floating nodes, the cracked element transforms into sub-elements, facilitating separate integration of each sub-element. A smoothing cell-based integration technique is employed to convert the area integral to line integral which mitigates the element distortion issues. The temperature distribution is initially determined across the entire domain, and then imposed as thermal loads in the 2D domain. The thermal stress intensity factor is calculated for both homogeneous and bi-material specimens using the interaction energy integral approach, and the crack propagation is predicted using circumferential stress criterion. The accuracy of the proposed framework is demonstrated with several benchmark problems of fracture mechanics. The develop framework yields comparable results with the available literature with less modeling complexity.
50.	NCCP collisions with para-H2: Accurate potential energy surface and quantum dynamics at interstellar temperatures **Ritika, TJD Kumar** - Monthly Notices of the Royal Astronomical Society, 2024 **Abstract:** The effect of para-hydrogen (jp = 0) collisions on the rotational de-excitation transitions of molecule NCCP is investigated in this study. The scattering information is obtained by spherically averaging a four-dimensional potential energy surface (4DPES) over various H2 molecule orientations. The calculations used the CCSD(T)-F12a method and aug-cc-pVTZ basis set to generate a 4DPES for the NCCP-H2 van der Waals system. Within the NCCP-para-H2 4DPES, a minimum energy point of 191.82 cm-1 is attained at a distance of 3.6 Å from the centre of mass of H2 and NCCP. To compute cross-sectional data for NCCP interacting with para-H2 (jp = 0), close coupling calculations are employed, encompassing total energies up to 600 cm-1. The resulting rate coefficients [)] are calculated across a temperature range spanning from 5 K to 200 K. In accordance with propensity, even Δj =-2 transitions are highly preferred. Comparatively, the derived) for NCCP-H2 are determined to be 1.5-4.5 times of NCCP-He. This observation implies that relying on a scaling factor of 1.38 to extrapolate rate coefficients for H2 collisions from those of NCCP-He is not a reliable approach.
51.	Noise impact on optimum parameter for signal deconvolution A Gupta, **CC Reddy** - IETE Journal of Research, 2024 **Abstract:** In many areas, such as speech processing, communication, and measurement systems, where the actual signal is not directly available, Wiener deconvolution is a widely used signal restoration technique. The accuracy of the estimated signal in Wiener deconvolution is determined by the unknown filter parameter. To compute this unknown parameter, complex and time-consuming numerical as well as iterative computation approaches were proposed in the literature, which also often compute an unoptimized unknown filter parameter. To address the computational problem and estimate a more accurate unknown filter parameter, the authors reported an analytical solution in a prior work for a given signal to noise ratio. However, it was revealed that the actual optimum parameter value also varies with noise also. In this paper, the authors propose a new analytical solution for optimum parameter estimation that includes noise as well. The authors compared the modified analytical solution to existing numerical computation methods for different values of Signal to Noise Ratio and demonstrated that the proposed

	methods' optimum parameter estimation is always close to the actual optimum value, which resulted in more accurate signal deconvolution. Proposed mathematical solutions are also verified with experimental signals, acquired in a laboratory.
52.	Novel air-cooling strategies for large capacity radiant air-conditioning units driven by absorption systems **G Singh, R Das** - Solar Energy, 2024 **Abstract:** Three novel air-cooling strategies/designs are introduced for solar and biogas/natural gas aided high capacity radiant absorption-cooling systems (RACS) varying between 100 and 121 tons, when these are integrated with desiccant ventilation unit (DVU). For all of the proposed strategies, the radiant system is operated solely with vapor absorption chiller. In the first design, there is a compressor driven direct expansion cooling coil and compression chiller operated chilled water cooling coil (CWCC). In the second design, there is an indirect evaporative cooler and combined compression and absorption-based CWCC. In the third design, a heat recovery unit (HRU) and combined compression and absorption-based CWCC are included. The presented work addresses a 5000 m2 building situated in hot-humid climate to portray characteristics of the proposed techniques that can be used in the RACS. In the studied designs, solar energy intermittency has been partially addressed by including a gas-fired boiler in conjunction along with solar collectors. Further system deficiency in supplying heat energy has been addressed by using electrical heating. Results ensure 25.4 % of energy savings with the third design against the first design. The maintained thermal comfort conditions vary between 22 °C and 26 °C with relative humidity between 40 % and 61 %. It is also observed that the HRU reduces the net thermal energy requirement at the desiccant regeneration side by 29.8 %. It is envisaged that due to available roof space constraint for solar collectors, compression chiller in the DVU cannot be fully eliminated in large cooling capacity office buildings.
53.	Nucleation kinetics of ascorbic acid in various aqueous solvents **J Yadav,** T Kendall…**SA Patel** - Industrial and Engineering Chemistry Research, 2024 **Abstract:** The nucleation kinetics of ascorbic acid in water and binary solvent systems of ethanol–water and isopropanol–water have been analyzed by the classical nucleation theory. For that, in total, 3065 data of induction time were collected by the isothermal method at five supersaturations in each solvent system. The induction time data are well represented with the Poisson probability distribution to determine the nucleation rate (J) and growth time (tg). The nucleation rate is found to be highest in water (1319.87 m–3 s–1) and decreases with increasing the alcohol composition in the binary solvent systems, showing the minimum nucleation rate (179.24 m–3 s–1) in the isopropanol−water system with a 0.6/0.4 mole fraction ratio. Furthermore, the kinetic parameter (A) decreases, whereas the thermodynamic parameter (B) increases with an increase in the alcohol composition in the aqueous solvent system. The interfacial energy (γ), critical radius (rc), and Gibbs free energy (ΔGc) were observed to be high for solvent systems with higher alcohol composition, which indicates a lower interaction between the solute and solution due to high interfacial tension. 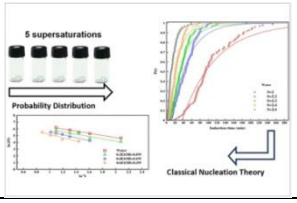
54.	On arithmetic nature of a -Euler-double zeta values **T Chatterjee, S Garg** - Proceedings of the American Mathematical Society, 2024 **Abstract:** Chatterjee and Garg [Proc. Amer. Math. Soc. 151 (2023), pp. 2011-2022] established closed form for a -analogue of the Euler-Stieltjes constants. In this article, we aim to build upon

	their work by extending it to a -analogue of the double zeta function. Specifically, we derive a closed form expression for which is a -analogue of Euler's constant of height and appear as the constant term in the Laurent series expansion of a -analogue of the double zeta function around and. Moreover, we examine the linear independence of a set of numbers involving the constant , where for any integer , that appears in the Laurent series expansion of a -double zeta function. Finally, we discuss the irrationality of certain numbers involving a -double Euler-Stieltjes constant.
55.	Optimal control problem governed by wave equation in an oscillating domain and homogenization L Faella, **R Raj, BC Sardar** - Journal of Applied Mathematics and Physics, 2024 **Abstract:** In this article, we consider the optimal control problem governed by the wave equation in a 2-dimensional domain Ω in which the state equation and the cost functional involves highly oscillating periodic coefficients A and B, respectively. This paper aims to examine the limiting behavior of optimal control and state and identify the limit optimal control problem, which involves the influences of the oscillating coefficients.
56.	Optimized dataset generation and disturbance rejection methodology for neural network controllers in second-order systems **AH Kumar, AVR Teja** - 2023 IEEE International Conference on Power Electronics, Smart Grid, and Renewable Energy (PESGRE), 2024 **Abstract:** Performance of a Neural Networks is highly dependent on the dataset provided it to learn. Traditionally, Neural Networks were used as tools to aid existing controller's performance or they were trained using existing controllers such as Proportional-Integral (PI) or Sliding Model Controller's data hence limiting its performance and accuracy to that of the controller itself. In this paper, an ideal dataset that gives the best desirable response is derived theoretically and used to train the neural controllers thus enhancing its performance much better than traditional PI controllers. The paper also proposes a control methodology by using multiple neural networks to reject the disturbance coming into the system and mitigate it easily much faster than the PI controllers with no overshoots. Detailed theoretical derivations are provided for the dataset generation and proposed methodology. The viability of the proposed neural controller was simulated and trained in MATLAB/Simulink environment and its response to variation in reference input has been inferred. The performance comparisons are made with the PI controller data and presented.
57.	Parallel governing criteria for non-Newtonian droplet rebound suppression on superhydrophobic surfaces **K Kamaluddin**, GC Pal, P Dhar, **CS Sharma, D Samanta** - Colloids and Surfaces A: Physicochemical and Engineering Aspects, 2024 **Abstract:** Non-Newtonian droplets are known to suppress rebound on superhydrophobic (SH) surfaces. Our previous work (Dhar et al., Phys Rev Fluids, 2019, vol 4 [1]) showed that the polymer concentration and impact velocity must exceed a certain threshold to initiate the onset of rebound suppression. Analogous to drag reduction or elastic instabilities, we proposed that rebound suppression occurs only when the Weissenberg number exceeds unity (i.e., Wi >1) at the onset of retraction. In this study, we explore four different types of SH surfaces to examine the universality of the previous observation (the importance of Wi >1 for rebound suppression). We observed that rebound suppression does not occur on all types of SH surfaces. The surfaces where rebound suppression was observed are categorized as 'Type-I', while the remaining as 'Type-II'. The non-uniformity in the rebound suppression phenomena is explained by the role of Cassie to Wenzel transformation (CWT) or impalement. We showed that for 'Type-I' surfaces, when the ratio of dynamic pressure (PD) to minimum capillary pressure (PC) exceeds unity (i.e., PD/PC > 1), the rebound is suppressed. The 'Type-II' surfaces have characteristic spacing in the

	order of nanometers, which is three orders of magnitude lower than the microtextured ‘Type-I’ surfaces. Thereby, the minimum capillary pressure is significantly higher for ‘Type-II’ surfaces. The dynamic pressure could not surpass the minimum capillary pressure for the impact velocities and polymer concentrations studied for the ‘Type-II’ surfaces. As PD/PC remained < 1, for ‘Type-II’ surfaces, rebound suppression was not observed. It must be noted that for the same values of PD/PC > 1 values, water droplets didn’t show rebound suppression on ‘Type-I’ surfaces. The non-Newtonian droplets are known to slow down the retraction dynamics due to normal stress, extensional viscosity and higher adsorption at the substrate. We have demonstrated the role of extensional viscosity in this study, particularly how strain stiffening of radial filaments emanating from the droplet aids in dissipating energy, which further aids in arresting drop rebound. Therefore, the existence of two parallel mechanisms: the role of fluid elasticity (manifested through Wi > 1), and the role of CWT or impalement (manifested through PD/PC > 1), are necessary conditions for non-Newtonian drop rebound suppression on superhydrophobic surfaces. 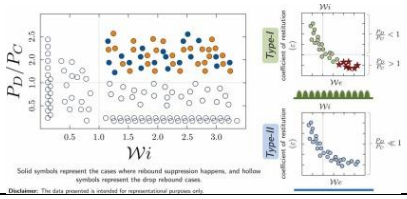
58.	Performance investigation of solar energy–aided compression-based building air conditioning strategies for variable climatic regions **G Singh, R Das** - Environmental Science and Pollution Research, 2024 **Abstract:** Decoupling cooling and ventilation tasks with an existing air conditioning methodology are a promising performance-enhancement technology. In this direction, different configurations of a desiccant-integrated independent ventilation element attached to a conventional cooling system are proposed in this study. This work establishes a quantitative comparative performance analysis among the different process air cooling (obtained through desiccant dehumidification) techniques for three different climates, namely, hot-dry, tropical, and Mediterranean. EnergyPlus simulations have been executed on a small-scale office building of 400-m2 area. The building constructional details and other required simulation input parameters follow benchmark standards. As the chemical dehumidification increases, the process air, i.e., supply air temperature that cannot be sent directly to the room, needs to be cooled. Three approaches for process air cooling have been considered: direct expansion (DX) cooling coil, indirect evaporative cooling (IEC), and sensible heat recovery wheel (SHRW). A solar collector assembly with a supporting heating arrangement is coupled with desiccant unit for regeneration. Outdoor air is used for regeneration in the case of the DX cooling coil and IEC, whereas return air is used in the heat recovery wheel case. Annual simulation results reveal that the SHRW-aided case performs superior than DX coil case for the pertinent climatic conditions, with 9.6 to 45.01% of annual energy savings. For the IEC, energy consumption was 1.8 to 18.38% less than that of DX coil. Also, using return air in this best-suited case reduces the net thermal energy requirement for regeneration by 14.63 to 71.65% with respect to DX coil.
59.	Present, past, and future of lean six sigma applications: from evolution to the era of artificial intelligence AB Singh, G Gaurav, **P Sarkar**,… - Recent Patents on Engineering , 2024 **Abstract:** Background: Lean Six Sigma is a fact-based, data-driven approach that avoids mistakes to improve quality and efficiency. Artificial intelligence (AI) is now evident in lean six sigma appli-cations. AI waste elimination solutions can eliminate large amounts of waste that LSS could not. In lean six sigma, six sigma tackles process variance, whereas lean reduces waste to improve process quality and efficiency. Objective: To describe new pieces, trends, and the

	adoption and implementation of new technologies like AI by examining the current literature across multiple aspects for a more instructive and piquant viewpoint. Methods: This study is a combination of systematic and bibliometric review, where the systematic review was based on a class framework by selecting 97 articles from reputed journal databases, and the bibliometric review was conducted using a VOS viewer and web of science database for a peri-od of 15 years (2007-2022). Results: By describing LSS's historical evolution, major concerns, prevalent research approaches, and application areas, the study helps practitioners and academics understand its present state for robust research. AI and other cutting-edge technologies help discover non-value-added operations that are difficult to recognize manually. Conclusion: This study has revealed the critical success factors for deploying LSS in numerous businesses. The motivations, barriers, and limits in the direction of the application of LSS are also discussed. The research trends in implementing modern technologies like AI showed a green wave. Future research may emphasize and dominate LSS implementation issues with modern technologies like AI.
60.	Quantitative analysis of hydropower potential in the upper Beas basin using geographical information system and MIKE 11 Nedbor Afrstromnings Model (NAM) **M Kumar, RK Tiwari**, K Kumar… - Ecohydrology, 2024 **Abstract:** The present study aims to identify potential locations for small-scale hydroelectric power (HEP) stations in hilly regions for the purpose of generating renewable energy. A rainfall-runoff (R-R) model of the Beas River catchment was established using the MIKE 11 NAM to estimate the available discharge. The model was calibrated and validated over the period of June-2015–May-2018 and June-2018–May-2020, respectively, using daily observed discharge data at the Pandoh Dam site. The model exhibited good performance with a coefficient of determination (R^2) of 0.82 during calibration and 0.70 during validation and a water balance of −0.01% and −18%, respectively. However, L_{max}, CK_1, CK_2 and CQOF are found most sensitive parameters during the calibration. Further, thirteen major streams of order five or higher were selected for the assessment of hydropower potential, resulting in the identification of 131 potential run-of-river (ROR) hydropower sites. The hydropower potential at two proposed sites, Bhang SHEP (9 MW) and Raison SHEP (18 MW), was estimated to be 11 and 15 MW, respectively, using 90% dependable flow. The results demonstrate the effectiveness of using Digital Elevation Model (DEM) and Geographic Information System (GIS) techniques for determining hydropower potential in ungauged basins in the Himalayas.
61.	Recent advances in energy-efficient chlorine production via HCl electrolysis A Kafle, D Gupta, S Mehta, K Garg, **TC Nagaiah** - Journal of Materials Chemistry A, 2024 **Abstract:** Chlorine (Cl2) is one of the most important and prime feeding reactants in the chemical industries, but around half of the chlorine employed in the industry gets converted into secondary products, mainly HCl. The conversion of HCl back to chlorine can be the best option for its maximum utilization. Although the catalytic conversion strategy is well established for the chemical recycling of chlorine, the drawbacks associated with it, such as the corrosion and stability of the catalyst, demand better alternatives. To overcome these issues, the electrolytic conversion of HCl for Cl2 and H2 generation is considered; however, high energy requirements and safety issues associated with this process call for its improvement. For this, the concept of replacing the cathodic hydrogen evolution reaction with the oxygen reduction reaction by introducing an oxygen depolarized cathode has been introduced as an energy-efficient and safe electrolysis approach. In this regard, this paper reviews the current trends in the efficient electrolysis of HCl, problems associated with it, and strategies employed to overcome it and puts forward its future perspectives.

	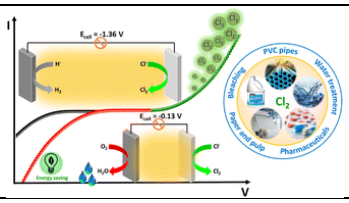
62.	Relationship between the variations in glacier features classified on a large scale with climate variables: a case study of Gangotri Glacier KV Mitkari, S Sofat…**RK Tiwari** - Environmental Monitoring and Assessment, 2024 **Abstract:** Changes in glacier area, glacial lakes, debris cover, and geomorphological features such as debris fans have a significant impact on glacial dynamics. Therefore, precise and timely observation and tracking of glacier surface changes is a necessity. The availability of high spatial resolution remote sensing images has made it viable to analyse the glacier surface changes at a local level. However, with an increase in spatial resolution, the spectral variability increases, giving rise to additional challenges (such as false changes and misregistration) in the change detection process. These challenges can preferably be dealt with using an object-based change detection (OBCD) approach rather than the conventional pixel-based change detection approach. Therefore, this study has proposed an OBCD methodology using high-spatial-resolution remote sensing images to detect changes in glacier features. Variability in glacier features has been further analysed by associating it with important climate variables, that is, air temperature and precipitation. As a case study, the changes in Gangotri Glacier (Uttarakhand Himalayas in India) features have been studied using high-spatial-resolution WorldView-2 and Linear Imaging Self-Scanning System (LISS)-4 images for a 3-year period 2011–2014. The spectral correspondences between glacier surface and non-glacier surface have been handled by considering brightness temperature and slope as ancillary data to improvise their distinction. A change detection accuracy of ~ 84% has been obtained using the OBCD approach. Results further show that the variations in glacier features are in congruence with the climatic observations.
63.	Remarkable enhancement of the adsorption and diffusion performance of alkali ions in two-dimensional (2D) transition metal oxide monolayers via Ru-doping S Sahoo, P Kumari ...**R Ahuja**… - Scientific Reports, 2024 **Abstract:** Transition metal oxides (TMO) are the preferred materials for metal ion battery cathodes because of their high redox potentials and good metal-ion intercalation capacity, which serve as an outstanding replacement for layered sulphide. In this work, using first-principles calculations based on Density functional theory approach, we explored the structural and electronic properties which comprise of adsorption and diffusion behaviour along with the analysis of voltage profile and storage capacity of Ru doped two-dimensional transition metal oxide , , and monolayers. The adsorption of alkali ions (Li, Na) to the surface of TMOs is strengthened by Ru-atom doping. Ru doping enhanced the adsorption energy of Li/Na-ion by 25%/11% for , 8%/13% for , and 10%/11% respectively. The open circuit voltage (OCV) also increases due to the high adsorption capacity of doped Monolayers. Ru doping makes the semiconducting TMOs conduct, which is suitable for battery application. As alkali ion moves closer to the dopant site, the adsorption energy increases. When alkali ions are close to the vicinity of doping site, their diffusion barrier decrease and rises as they go further away. Our current findings will be useful in finding ways to improve the storage performance of 2D oxide materials for application in energy harvesting and green energy architecture.
64.	Role of tungsten disulfide quantum dots in specific protein–protein interactions at air–water interface **H Kaur**, M Garg, **D Tomar**, S Singh, **KC Jena** - The Journal of Chemical Physics, 2024 **Abstract:** The intriguing network of antibody–antigen (Ab–Ag) interactions is highly governed

	by environmental perturbations and the nature of biomolecular interaction. Protein–protein interactions (PPIs) have potential applications in developing protein-adsorption-based sensors and nano-scale materials. Therefore, characterizing PPIs in the presence of a nanomaterial at the molecular level becomes imperative. The present work involves the investigation of antiferritin–ferritin (Ab–Ag) protein interactions under the influence of tungsten disulfide quantum dots (WS2 QDs). Isothermal calorimetry and contact angle measurements validated the strong influence of WS2 QDs on Ab–Ag interactions. The interfacial signatures of nano–bio-interactions were evaluated using sum frequency generation vibration spectroscopy (SFG-VS) at the air–water interface. Our SFG results reveal a variation in the tilt angle of methyl groups by ∼12° ± 2° for the Ab–Ag system in the presence of WS2 QDs. The results illustrated an enhanced ordering of water molecules in the presence of QDs, which underpins the active role of interfacial water molecules during nano–bio-interactions. We have also witnessed a differential impact of QDs on Ab–Ag by raising the concentration of the Ab–Ag combination, which showcased an increased inter-molecular interaction among the Ab and Ag molecules and a minimal influence on the methyl tilt angle. These findings suggest the formation of stronger and ordered Ab–Ag complexes upon introducing WS2 QDs in the aqueous medium and signify the potentiality of WS2 QDs relevant to protein-based sensing assays.
65.	SHE-MTJ based ReLU-max pooling functions for on-chip training of neural networks **V Vadde, B Muralidharan, A Sharma** - AIP Advances, 2024 **Abstract:** We present a detailed investigation of various routes to optimize the power consumption of the spintronic-based devices for implementing rectified linear activation (ReLU) and max-pooling functions. We examine the influence of various spin Hall effect layers, and their input resistances on the power consumption of the ReLU-max pooling functions, we also access the impact of the thermal stability factor of the free-ferromagnet layer on the power consumption and accuracy of the device. The design for ReLU-max pooling relies on the continuous rotation of magnetization, which is accomplished by applying orthogonal spin current to the free-FM layer. We also demonstrate the non-trivial power-resistance relation, where the power consumption decreases with an increase in SHE resistance. We utilize the hybrid spintronic-CMOS simulation platform that combines Keldysh non-equilibrium Green's function (NEGF) with Landau-Lifshitz-Gilbert-Slonzewski (LLGS) equations and the HSPICE circuit simulator to evaluate our network. Our design takes 0.343 μW of power for ReLU emulation and 17.86 μW of power for ReLU-max pooling network implementation at a thermal stability factor of 4.58, all while maintaining reliable results. We validate the efficiency of our design by implementing a convolutional neural network that classifies the handwritten-MNIST and fashion-MNIST datasets. This implementation illustrates that the classification accuracies achieved are on par with those attained using the ideal software ReLU-max pooling functions, with an energy consumption of 167.31 pJ per sample.
66.	Solar thermal energy storage systems based on discotic nematic liquid crystals that can efficiently charge and discharge below 0 °c **M Gupta, Ashy** - Advanced Energy Materials, 2024 **Abstract:** Solid-state solar thermal fuels (SSTFs) serve as efficient means of storing solar energy as chemical potential energy in a closed loop system and releasing it as heat on-demand. An ideal SSTF requires photoswitchability in visible-region without any external heating as well as extended storage times. However, existing systems often rely on ultraviolet (UV) light or heating for photoswitching, or suffer from low storage times. Addressing this, a novel strategy is presented to obtain visible-light responsive SSTFs designed to operate effectively at room-temperature or sub-zero temperatures by innovatively integrating a tetra-ortho-fluoro/chloro azobenzene arm in triphenylene based liquid crystal (LC) moiety. The resulting compounds exhibit discotic nematic (ND) mesophases till −6.5 °C. These compounds exhibit excellent photocyclability, photostability, and sufficient half-lives of cis states. Achieving up to 77%

	charging under sunlight with a bandpass filter and 62.4% without it, these systems uniquely demonstrate efficient chargeability and dischargeability at sub-zero temperatures. Upon discharging, temperature rise of up to 6.5 and 29.5 °C occur at room-temperature (25 °C) and sub-zero temperatures (around −6 to −7 °C), respectively. This efficacy is attributed to less-ordered ND phases providing conformational freedom for photoisomerization at low temperatures.
67.	Solvent directed morphogenesis of a peptidic-benzimidazolium dipodal receptor: ratiometric detection and catalytic degradation of ochratoxin A S Saini, A Sharma, N Kaur, **N Singh** - Analytical Methods, 2024 **Abstract:** Ochratoxin A (OTA) is the most abundant and harmful toxin found in agriculture and processed food. The environment and human health are both harmed by this mycotoxin. As a result, in various scenarios, selective detection and biodegradation of ochratoxin A are essential. The current study reveals the morphogenesis of a peptidic-benzimidazolium dipodal receptor (SS4) and its application as a catalytic and sensing unit for the detection and degradation of OTA in an aqueous medium. Initially, a facile and scalable method was executed to synthesize SS4, and solvent-directed morphogenesis were examined under SEM analysis. Consequently, molecular recognition properties of self-assembled architectures were explored using UV-visible absorption, fluorescence spectroscopy, and atomic force microscopy (AFM). The designed probe showed a ratiometric response for OTA and served as a catalytic unit for the degradation of OTA at a short interval of 25 min. The biodegradation pathway for OTA was accomplished using LC-MS analysis. Furthermore, the reliability of the developed method was checked by determining the spiked concentrations of the OTA in cereals and wine samples. The results obtained are in good agreement with the % recovery and RSD values. The present work provides a robust, selective, and sensitive method of detection and degradation for OTA. 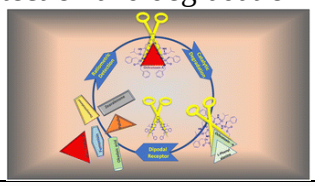
68.	Strong in-plane magnetization and spin polarization in (Co0.15Fe0.85)5GeTe2/graphene van der waals heterostructure spin-valve at room temperature R Ngaloy, B Zhao…**L Bainsla**... - ACS Nano, 2024 **Abstract:** Van der Waals (vdW) magnets are promising, because of their tunable magnetic properties with doping or alloy composition, where the strength of magnetic interactions, their symmetry, and magnetic anisotropy can be tuned according to the desired application. However, so far, most of the vdW magnet-based spintronic devices have been limited to cryogenic temperatures with magnetic anisotropies favoring out-of-plane or canted orientation of the magnetization. Here, we report beyond room-temperature lateral spin-valve devices with strong in-plane magnetization and spin polarization of the vdW ferromagnet (Co0.15Fe0.85)5GeTe2 (CFGT) in heterostructures with graphene. Density functional theory (DFT) calculations show that the magnitude of the anisotropy depends on the Co concentration and is caused by the substitution of Co in the outermost Fe layer. Magnetization measurements reveal the above room-temperature ferromagnetism in CFGT and clear remanence at room temperature. Heterostructures consisting of CFGT nanolayers and graphene were used to experimentally realize basic building blocks for spin valve devices, such as efficient spin injection and detection. Further analysis of spin transport and Hanle spin precession measurements reveals a strong in-plane magnetization with negative spin polarization at the interface with graphene, which is supported by the calculated spin-polarized density of states of CFGT. The in-plane magnetization of CFGT at room temperature proves its usefulness in graphene lateral spin-valve devices, thus revealing its potential application in spintronic technologies.

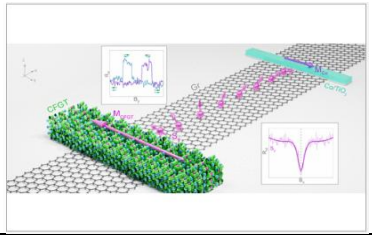

69. [Synthesis and evaluation of thermo-physical properties of hybrid Mg/SiC–Al2O3 composites for solar heat absorber]
M Singh, G Vinay…**H Singh** - Transactions of the Indian Institute of Metals, 2024

Abstract: The current study investigates the thermo-physical properties of the Mg-based hybrid composite produced via hot press sintering. The SiC and Al2O3 particulates were selected as reinforcement in the Mg matrix. The volume fraction of the matrix and the reinforcements is kept constant at 40:60. However, by varying the volume fraction ratio of SiC and Al2O3 five different composites were prepared, designated as Mg–10SiC50Al2O3, Mg–20SiC40Al2O3, Mg–30SiC30Al2O3, Mg–40SiC20Al2O3 and Mg–50SiC10Al2O3. The effect of SiC and Al2O3 reinforcement on thermal conductivity, specific heat capacity and density were evaluated. XRD analysis determined the formation of intermittent phases like Mg2Si and MgO in the Mg matrix composite, whereas SEM analysis confirmed an almost uniform distribution of the reinforcements in the Mg matrix. Among the developed composites, the highest thermal conductivity of 193.42 W/mK (for Mg–50SiC10Al2O3) and highest specific heat of 4.68 kJ/kg°C (for Mg–30SiC30Al2O3) were observed along with the relative density of 85–77%. The properties achieved by the developed composites are found to be aligned with the requirement of third-generation solar energy storage materials and could be used for thermal storage usage such as solar thermal applications.

70. [Synthesis of core–shell structured zeolite nanocomposite comprising ZSM-5 core and zeolite Y shell]
JH Advani, AK Manal, N Kanna…**R Srivastava** - Materials Letters, 2024

Abstract: Zeolite core-zeolite shell synthesis is promising to enhance selective catalysis in the petrochemical industry, yet the complex synthesis poses a challenge. The successful growth of the Na-Y zeolite shell over the ZSM-5 core, producing a nanocrystalline core–shell structure, was achieved by hydrothermal crystallization via a sequential seeding-dissolution-growth route via alkaline-induced desilication of ZSM-5, followed by the addition of silica and alumina precursors to grow nanosized Na-Y crystallites over the ZSM-5 core. The successful fabrication of the core–shell structure was confirmed by different physicochemical characterizations. The optimized core–shell zeolite demonstrated noteworthy characteristics, featuring a high BET surface area of 493 m2g−1 and an external surface area of 195 m2g−1. Further, the material exhibited a connected porous network, contributing to the total pore volume of 0.52 cm3g−1. Such a strategy can be adopted to fabricate other core–shell materials for advancing the catalytic processes.

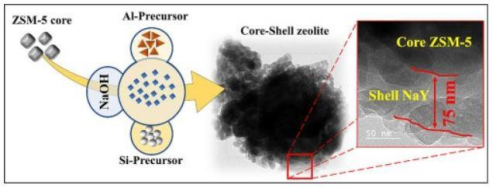

71. [The resurgence of old material: The impact of boehmite-derived catalytic material on the formation of dihydropyran compounds and its application to access fragrant derivatives]
M Barik, B Patel, **A Kumar, R Srivastava**… - Chemical Engineering Journal, 2024

Abstract: Bulk materials are the oldest in heterogeneous catalysis, but with the resurgence of

	recent interest, it has emerged as one of the best catalytic tools to unlock their full potential. Boehmite-derived alumina materials are widely studied for catalytic organic transformations. Despite the progress, understanding the mechanistic insights of its catalytic behaviour has remained obscure. Here, we demonstrate the catalytic performance of a boehmite-derived alumina material to a highly selective catalytic process for the preparation of dihydropyran compounds. The catalytic material displayed excellent activity in terms of conversion (up to 99%) and selectivity (up to 99%). The material was characterized using different techniques and observed that the γ-alumina phase with inherent mild acidic character are key feature for the catalytic activity. Based on NMR and in situ FT-IR spectroscopic investigations a probable mechanism is proposed. This study expands the application of robust material for the preparation of industrially important fragrance compounds. The scope of the catalytic study encompasses a range of substrates and scale-up activities. 
72.	The role of inflammatory mediators and matrix metalloproteinases (MMPs) in the progression of osteoarthritis **A Mukherjee, B Das** - Biomaterials and Biosystems, 2024 **Abstract:** Osteoarthritis (OA) is a chronic musculoskeletal disorder characterized by an imbalance between (synthesis) and catabolism (degradation) in altered homeostasis of articular cartilage mediated primarily by the innate immune system. OA degenerates the joints resulting in synovial hyperplasia, degradation of articular cartilage with damage of the structural and functional integrity of the cartilage extracellular matrix, subchondral sclerosis, osteophyte formation, and is characterized by chronic pain, stiffness, and loss of function. Inflammation triggered by factors like biomechanical stress is involved in the development of osteoarthritis. In OA apart from catabolic effects, anti-inflammatory anabolic processes also occur continually. There is also an underlying chronic inflammation present, not only in cartilage tissue but also within the synovium, which perpetuates tissue destruction of the OA joint. The consideration of inflammation in OA considers synovitis and/or other cellular and molecular events in the synovium during the progression of OA. In this review, we have presented the progression of joint degradation that results in OA. The critical role of inflammation in the pathogenesis of OA is discussed in detail along with the dysregulation within the cytokine networks composed of inflammatory and anti-inflammatory cytokines that drive catabolic pathways, inhibit matrix synthesis, and promote cellular apoptosis. OA pathogenesis, fluctuation of synovitis, and its clinical impact on disease progression are presented here along with the role of synovial macrophages in promoting inflammatory and destructive responses in OA. The role of interplay between different cytokines, structure, and function of their receptors in the inter-cellular signaling pathway is further explored. The effect of cytokines in the increased synthesis and release of matrix-decomposing proteolytic enzymes, such as matrix metalloproteinase (MMPs) and a disintegrin-like and metalloproteinase with thrombospondin motif (ADAMTS), is elaborated emphasizing the potential impact of MMPs on the chondrocytes, synovial cells, articular and periarticular tissues, and other immune system cells migrating to the site of inflammation. We also shed light on the pathogenesis of OA via oxidative damage particularly due to nitric oxide (NO) via its angiogenic response to inflammation. We concluded by presenting the current knowledge about the tissue inhibitors of metalloproteinases (TIMPs). Synthetic MMP inhibitors include zinc binding group (ZBG), non-ZBG, and mechanism-based inhibitors, all of which have the potential to be therapeutically beneficial in the treatment of osteoarthritis. Improving our understanding of the signaling pathways and molecular mechanisms

	that regulate the MMP gene expression, may open up new avenues for the creation of therapies that can stop the joint damage associated with OA. 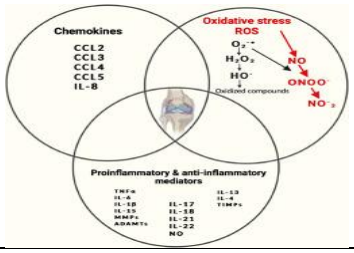
73.	The role of occupancy on traffic flow in a multiple-loop network M Verma, T Singla, **AK Gupta**… - Physica A: Statistical Mechanics and its Applications, 2024 **Abstract:** A dynamic model for traffic flow is proposed to analyze the impact of occupancy in a multiple-loop network with a single intersection. The graph representation of multiple-loop lines is obtained utilizing the cell-transmission model, and consequently, the density equations are derived. The macroscopic fundamental diagrams are investigated for different cases of occupancy and the fraction of vehicles. For the double-loop lines, equilibrium densities, traffic currents, and travel time are obtained theoretically and validated via simulation. It is observed that the equilibrium densities increase linearly against the mean density for an equal fraction of vehicles while the traffic currents remain symmetric, unlike the case of an unequal fraction of vehicles. The travel time varies inversely with respect to the occupancy of the loop line. Additionally, when the fraction of vehicles and occupancy at both nodes are different, a critical value of mean density is obtained below (above), in which the travel time at one node is less (more) than the other. To analyze the traffic flow on multiple-loop lines, stability analysis is conducted using the tools from cooperative theory and repelling boundaries. As a result, the vehicular densities converge to a unique equilibrium point irrespective of the initial densities in the multiple-loop network. The theoretical results agree well with the simulation results.
74.	Totally asymmetric simple exclusion process with local resetting in a resource-constrained environment **N Bhatia, AK Gupta** - Physical Review E, 2024 **Abstract:** Inspired by the process of mRNA translation, in which the stochastic degradation of mRNA-ribosome machinery is modeled by the resetting dynamics, we study an open totally asymmetric simple exclusion process with local resetting at the entry site in a resource-constrained environment. The effect of constrained resources on the stationary properties of the system has been comprehended in the form of the filling factor. The mean-field approximations are utilized to obtain stationary state features, such as density profiles and phase diagrams. The phase diagram possesses pure phases as well as coexisting phases, including a low-density–high-density phase separation, which did not manifest under periodic boundary conditions despite the system being closed there as well. The role of the resetting rate has been investigated on the stationary properties of the system, depending on how the filling factor scales with the system size. In contrast to the resetting model for infinite resources, two distinct phase transitions are observed for the smaller values of the filling factor leading to a change in the topology of the phase diagram. The impact of the resetting rate along with the finite-size effect has also been examined on the shock dynamics. All the mean-field results are found in remarkable agreement with the Monte Carlo simulations.
75.	Understanding the role of surface charge on nanobubble capillary bridging during particle–particle interaction **N Dutta** , S Mitra**, N Nirmalkar** - Langmuir, 2024 **Abstract:** The interactions between particles due to long-range hydrophobic forces have been extensively investigated. The hydrophobic force is likely a capillary force that arises from the

	formation of capillary bridges due to the merging of nanobubbles. In this study, we aim to investigate the impact of the nanobubble surface charge on the capillary bridge and, subsequently, the interaction between particles. The surface charge of the nanobubbles was altered in the presence of various surfactants (cationic, anionic, and nonionic) and salts (mono-, di-, and trivalent). The particle–particle interaction was quantified by measuring the aggregate size of the hydrophobized glass particles. Both experimental and theoretical findings confirm that the interaction between particles was enhanced when the surface potential of the nanobubble was around the neutral regime. This is probably because, when the surface potential was close to neutral, the interaction between two surface-deposited nanobubbles dominated over electrostatic repulsion, which was more conducive to the formation of the nanobubble capillary bridge. The estimation of the constrained Gibbs potential also showed the capillary bridge to be more stable when surface charge density along the bridge gas–liquid interface was minimal. 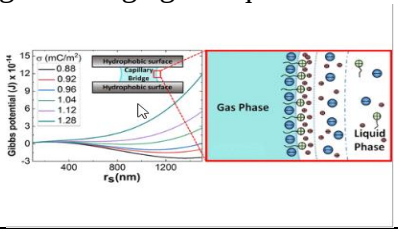
76.	Van Hove singularity driven enhancement of superconductivity in two dimensional Tungsten monofluoride (WF) **P Jamwal, R Ahuja, R Kumar** - Journal of Physics: Condensed Matter, 2024 **Abstract:** Superconductivity in two-dimensional materials has gained significant attention in the last few years. In this work, we report phonon-mediated superconductivity investigations in monolayer Tungsten monofluoride (WF) by solving anisotropic Migdal Eliashberg equations as implemented in EPW. By employing first-principles calculations, our examination of phonon dispersion
spectra suggests that WF is dynamically stable. Our results show that WF has weak electron-phonon coupling weak electron-phonon coupling strength (λ) of 0.49 with superconducting transition temperature (Tc) of 2.6 K. A saddle point is observed at 0.11 eV below the Fermi level (EF) of WF, which corresponds to the Van Hove singularity (VHS). On shifting the Fermi level to the VHS by hole doping (3.7 × 1014 cm−2), the electron-phonon coupling strength increases to 0.93, which leads to an increase in the Tc to 11 K. However, the superconducting temperature of both pristine and doped WF increases to approximately 7.2 K and 17.2 K, respectively, by applying the Full Bandwidth (FBW) anisotropic Migdal-Eliashberg equations. Our results provide a platform for the experimental realization of superconductivity in WF and enhancement of the superconducting transition temperature by adjusting the position of EF to the VHS.

Disclaimer: This publication digest may not contain all the papers published. Library has compiled the publication data as per the alerts received from Scopus and Google Scholar for the affiliation “Indian Institute of Technology Ropar” for the month of February, 2024. The author(s) are requested to share their missing paper(s) details if any, for the inclusion in the next publication digest.